Synthesis, Spectral Characterization, Catalytic and Antimicrobial Activities of Pd(II) and Ni(II) Schiff Base Complexes

Shahrul Nizam Ahmad[1]*, Thaigarajan Parumasivam[2], Nur Husnina Nasaruddin[1] and Siti Solihah Khaidir[1]

[1]Faculty of Applied Sciences, Universiti Teknologi MARA, 40450 Shah Alam, Selangor, Malaysia
[2]School of Pharmaceutical Sciences, Universiti Sains Malaysia, Minden 11800, Penang, Malaysia
*Corresponding author (e-mail: shahruln@uitm.edu.my)

Palladium(II) and nickel(II) complexes derived from aromatic Schiff bases were synthesized and characterized through physicochemical and spectroscopic analyses, viz., melting point, elemental analysis, molar conductivity, magnetic susceptibility, FTIR, UV-Vis, and ^{1}H and ^{13}C NMR. The shift in ν(C=N) to a lower frequency in FTIR of about 10 cm^{-1} indicated that complexation to Pd(II) and Ni(II) through the azomethine N was established. This was supported by the shifting of the azomethine proton signal to downfield and upfield regions in ^{1}H NMR. In addition, the shifting of the n−π*(C=N) band in the UV-Vis spectra, with Δλ = 20−47 nm, indicated involvement of the azomethine nitrogen in the complexation. Palladium(II) complexes performed better than nickel(II) complexes as catalysts in the copper-free Sonogashira reaction, with 100 % conversion of iodobenzene in 3 hours. In the antibacterial study, L1Me showed the most promising anti-MRSA and anti-MSSA activities, with both MIC and MBC values of 3 µg/ml against the tested strains. These findings highlight the potential of Pd(II) and Ni(II) complexes as catalysts and anti-microbial agents.

Keywords: Antibacterial; nickel; palladium; Schiff base; Sonogashira

Received: July 2023; Accepted: January 2024

Condensation of primary amines with ketones or aldehydes under specific conditions lead to the formation of compounds containing azomethine groups, which are widely recognized for their facile synthesis [1]. The Salen ligand system is a Schiff base ligand. and one of the most studied groups of chelate ligands [2]. It was originally termed for the family of a bisimine compound, N,N′-bis(salicylidine)ethylene-diamine, derived from salicylaldehyde and ethylenediamine in a 2:1 molar ratio [3-4]. The earliest report of salen-metal complexes was published by Pfeiffer *et al.* in 1933 [2]. Various structural modifications have been made to this scaffold to expand its properties in the fields of pharmaceuticals, catalysis, material chemistry, and coordination chemistry [5].

Pd(II) and Ni(II) complexes derived from Schiff base ligands have received significant attention due to their unique properties and potential applications in catalysis and antimicrobial therapy. Palladium complexes are widely used in synthesis and have become one of the most powerful and convenient C−C and C−N bond formation processes in pharmaceutical, materials, and synthetic chemistry [6]. Since they are able to catalyse under a non-harsh reaction atmosphere, produce high yields, and possess an exceptional level of stereo-, regio-, and chemo-selectivity, they have been used as catalysts in chemical reactions, particularly carbon-carbon coupling [7-8]. Nickel, another member of the same group as palladium, is less expensive and less toxic [9, 10]. Furthermore, the relatively more electro-positive nature of Ni allows for easier oxidative addition and slower β-hydride elimination due to the higher Ni−C bond rotation energy barrier compared to Pd [11]. Therefore, nickel complexes have attracted the attention of chemists as catalysts for C−C coupling reactions. Beletskaya and co-workers were the first to report on the use of Ni complexes as catalysts for the Sonogashira coupling reaction in 2003 [11].

Antibiotics have significantly reduced the occurrence of infectious diseases and saved lives. However, there is still an urgent need for new anti-bacterial compounds to overcome newly emerging antibiotic resistance cases [12]. Therefore, many studies have been done on the antibacterial activities of metal complexes for the treatment of resistant cases. When compared to other transition metal species, metals from Group 10 have relatively high MICs [13]. Recently, Nyawade et al. reported on the antibacterial effects of new 2-pyrral amino acid Schiff base palladium(II) complexes against six species (Gram-positive, such as *Staphylococcus aureus*, Methicillin Resistant *Staphlococcus aureus* (MRSA), *Staphylococcus epidermidis*, *Streptococcus pyogenes*, and Gram-negative, such as *Pseudomonas aeruginosa* and *Klebsiella pneumonia*). One of the complexes showed high activity and comparable antimicrobial potency to ampicillin against MRSA, *S. epidermidis* and *S.*

pyogenes [14]. Meanwhile, Raj and his co-workers reported that the MIC values of nickel(II) Schiff base complexes against *S. aureus* was comparable to the standard drug, ciprofloxacin. The complexes also showed good MICs against MRSA [15-16].

Overall, this study comprehensively investigates Pd(II) and Ni(II) complexes derived from aromatic tetradentate Schiff base ligands. The complexes were tested as catalysts in copper-free Sonogashira reactions. For the antimicrobial study, several ligands and complexes were screened against MRSA ATCC 43300, MRSA NCTC 12494 and Methicillin Sensitive *Staphlococcus aureus* (MSSA) ATCC 12600. The results of this study could contribute to the development of new and effective catalysts and antimicrobial agents.

EXPERIMENTAL

Chemicals and Materials

Ethanol, acetonitrile, dimethyl sulfoxide (DMSO), ortho-phenylenediamine, salicylaldehyde, 5-fluorosalicylaldehyde, 5-chlorosalicylaldehyde, 5-methylsalicylaldehyde, 5-methoxysalicyladehyde and 5-nitrosalicylaldehyde were purchased from commercial suppliers and used as supplied, without further purification.

Characterization Methods

The micro-analytical data (C, H, and N) of all ligands and complexes were obtained using a Thermo Scientific Flash 2000 Elemental Analyser. Melting points were determined with a Stuart SMP10. A Perkin-Elmer Spectrum One FTIR spectrometer was employed to record infrared (IR) spectra of ligands and complexes between 450–4000 cm^{-1} using KBr pellets. ^{1}H and ^{13}C NMR spectra of the samples were recorded on a Bruker Varian 600 MHz spectrometer with $CDCl_3$ and DMSO-d_6 as solvents, and expressed in parts per million (δ, ppm). The magnetic susceptibility of the palladium(II) and nickel(II) complexes was measured using a Sherwood Auto Magnetic Susceptibility Balance. The molar conductivity of the complexes was determined using a Mettler Toledo Inlab 730 conductivity meter in a 10^{-3} M DMSO solution.

General Synthesis of L1 Ligands

The synthesis of L1 ligands has been reported in previous journals [17]. Approximately 10 mL of a hot ethanolic solution of ortho-phenylenediamine, OPD (1 mmol) was added to a stirred solution of salicylaldehyde derivatives (2 mmol) in absolute ethanol (5 mL) (**Scheme 1**). The solution was refluxed for 4 hours before being cooled and chilled overnight at approximately 4 °C. The coloured solid obtained was filtered, washed with cold ethanol, and then air-dried. Yield: L1H (56.0 %), L1F (79.3 %), L1C (78.7 %), L1M (71.8 %), L1OMe (79.2 %), L1N (92.1 %).

General Synthesis of Pd(II) Complexes

In a round bottom flask, 1 mmol of palladium(II) acetate was dissolved in 10 mL of acetonitrile. Separately, 1 mmol of ligand was dissolved in 10 mL of acetonitrile. The ligand solution was added dropwise into the flask containing the metal solution before being refluxed for 6 hours. The coloured solid that formed was then filtered, washed with a small quantity of cold acetonitrile, and air-dried. Yield: PdL1H (86.0 %), PdL1F (93.4 %), PdL1C (83.3 %), PdL1M (66.0 %), PdL1OMe (85.1 %).

General Synthesis of Ni(II) Complexes

In a round bottom flask, 1 mmol of nickel(II) acetate tetrahydrate was dissolved in 10 mL of ethanol. Separately, 1 mmol of ligand was dissolved in 10 mL of ethanol. The ligand solution was added dropwise to the flask containing the metal solution. The mixture was refluxed for 6 hours. The solid was then filtered, washed with a small amount of cold ethanol, and air-dried. Yield: NiL1H (74.7 %), NiL1F (93.8 %), NiL1C (83.9 %), NiL1M (76.3 %), NiL1OMe (74.0 %).

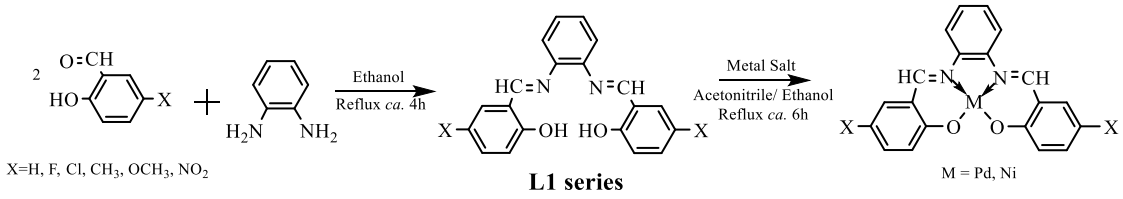

Scheme 1. Synthesis of Pd(II) and Ni(II) Schiff base complexes.

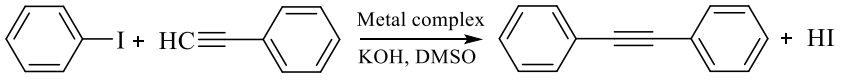

Scheme 2. The Sonogashira reaction procedure.

Sonogashira Reaction

A round bottom flask was charged with iodobenzene (1.0 mmol), phenylacetylene (1.5 mmol), metal complex (0.02 mmol) and KOH (2.0 mmol), and stirred under aerobic conditions with 7 mL of DMSO (**Scheme 2**). The mixture was heated at 140 °C for 12 hours and monitored every 3 hours using a Gas Chromatograph-Flame Ionization Detector (GC-FID) model Agilent 6890N to determine the percentage conversion of iodobenzene, as calculated using equation 1:

$$\% \text{ Conversion} = (A_{int} - A_{final})/A_{int} \quad (1)$$

where A_{int} is the peak area of iodobenzene before reaction and A_{final} is the peak area of iodobenzene after reaction.

Antibacterial Study

Bacterial Strains

MRSA ATCC 43300, MRSA NCTC 12493 and MSSA ATCC 12600 were purchased from American Type Culture Collection, USA.

Determination of Minimum Inhibitory Concentration (MIC) and Minimum Bactericidal Concentration (MBC)

The pre-weighed drugs were dissolved in DMSO and further diluted in a fresh Muller Hinton Broth (MHB) medium to reduce the concentration of DMSO to below 1 % (v/v).

The microdilution assay was performed using 96-well plates. Briefly, 100 µL of fresh MHB was added into all wells followed by the drug solution into row A in triplicate. A two-fold serial dilution was performed by transferring 100 µL from row A to B using a multichannel pipette. This step was repeated until row H and the excess 100 µL mixture from row H was discarded. 100 µL of diluted standardized log-phase bacterial suspension was added into the wells. The final volume in each well was 200 µL. The concentration of the drug ranged between 1.56 and 200 µg/mL, with vancomycin included as a positive control. The plate was incubated for 18 to 22 hours at 37 ˚C. Upon incubation, 50 µL of freshly prepared INT solution was added into all wells and re-incubated for 2 hours at 37 ˚C. The MIC is defined as the lowest drug concentration which prevented a colour change of the INT from colourless to pink. Prior to addition of the INT dye, 10 µL of the mixture was inoculated into Muller Hinton agar (MHA) plates to determine the MBC. The plates were incubated at 37 ˚C for 18 to 22 hours. The MBC was determined as the lowest drug concentration which did not produce any bacterial growth on the agar plate.

RESULTS AND DISCUSSION

Synthesis of Schiff Bases and their Pd(II) and Ni(II) Complexes

The condensation reaction between salicylaldehyde derivatives and OPD (1:2) in EtOH resulted in moderate to good yields of product (56.0 - 92.1 %). Equimolar complexation reactions between the ligands and palladium(II) acetate afforded moderate to good yields of palladium(II) complexes (66.0 - 86.0 %). Meanwhile, for the nickel(II) complexes, yields were in the range of 74.0 - 93.8 %. The ligands were all coloured yellow or orange, which is a common colour for compounds with C=N chromophores. The colours of the metal complexes of the L1 series were red, dark red and brown. The ligands were soluble in all organic solvents while the metal complexes were insoluble in common organic solvents, i.e., ethanol, methanol, chloroform and acetonitrile, but soluble in DMSO. All compounds existed as solids at room temperature and were stable towards air and moisture.

The micro-elemental data of the compounds are reported in **Table 1**. The percentage of C, H and N were in concordance with the proposed structure in Scheme 1. The melting points of all complexes were above 300 °C, which were higher than those of their parent ligands. This is due to the increase in molecular weight by the addition of palladium(II) and nickel(II) ions with strong dative covalent and ionic bonds between the ligands and metal ions.

The magnetic properties of the complexes were used to investigate the number of unpaired electrons in the partially filled *d*-orbitals. These measurements shed some light on the electron configuration of the metal ion in the complexes [18-19]. Magnetic susceptibility values of the complexes were all found to be 0 B.M. at room temperature, signifying that there were no unpaired electrons in the *d* orbital. This suggests a square planar geometry around the Pd(II) or Ni(II) central metal ions in the complexes. The DMSO solution of the complexes showed no significant conductivity indicating that they were non-electrolytic [20-21], containing no free ions.

Table 1. Physicochemical data for the ligands and complexes.

Compounds	Percent yield (%)	Elemental analysis % calculated (found)		
		C	H	N
PdL1H	86.0	54.38 (**55.23**)	3.17 (**3.06**)	6.76 (**7.38**)
NiL1H	74.7	64.40 (**63.93**)	3.78 (**3.76**)	7.51 (**6.95**)
PdL1F	93.4	52.59 (**52.19**)	2.65 (**2.59**)	6.13 (**6.77**)
NiL1F	93.8	58.73 (**58.89**)	2.96 (**2.76**)	6.85 (**6.88**)
PdL1C	83.3	49.06 (**50.53**)	2.47 (**2.59**)	5.72 (**6.05**)
NiL1C	83.9	54.36 (**55.81**)	2.74 (**2.89**)	6.34 (**6.40**)
PdL1M	66.0	58.88 (**59.40**)	4.04 (**4.04**)	6.24 (**6.39**)
NiL1M	76.3	65.88 (**65.32**)	4.52 (**4.47**)	6.98 (**6.81**)
PdL1OMe	85.1	54.96 (**53.97**)	3.77 (**3.65**)	5.83 (**6.37**)
NiL1OMe	74.0	61.01 (**60.94**)	4.19 (**4.14**)	6.47 (**6.42**)

Spectral Data

FT-IR Spectra

FT-IR data of the Pd(II) and Ni(II) complexes are tabulated in **Table 2** and their spectra are shown in **Figure 1** and **Figure 2,** respectively. The IR data for the ligands were reported previously [17], [23]. The main peak of azomethine, ν(C=N) was found in the range of 1612–1619 cm^{-1} in all the spectra of the free ligands. These peaks experienced a shift to lower frequencies in the range of 1606–1609 cm^{-1} and 1602–1609 cm^{-1} in the palladium(II) and nickel(II) complexes, indicating that complexation has been established through bonding of the azomethine nitrogen and metal centres [24-26]. $\Delta\nu_{(ligand\text{-}complex)}$ was ~10 cm^{-1}. The C=N bond became weaker upon complexation as a result of the inductive effect of the lone electron pair on the azomethine nitrogen being shared with the metal centre. This phenomenon was supported by the shifting of C–N peaks in all metal complexes [27].

The vibration of the hydroxyl group ν(OH), was found as a weak peak at 3222–3241 cm^{-1} in the ligands. Noticeably, these peaks disappeared in all metal complexes signalling that complexation was established between oxygen and metal centres through deprotonation of the hydroxyl group [21, 28]. The shifting of ν(C–O) in metal complexes further supported the establishment of a new bond between the metal centre and phenolic oxygen [29].

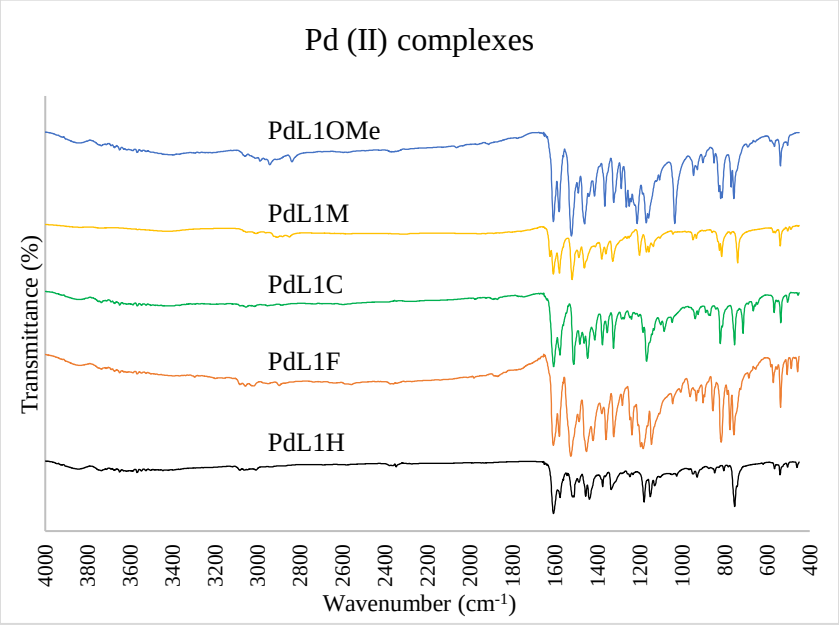

Figure 1. IR spectra of Pd (II) complexes.

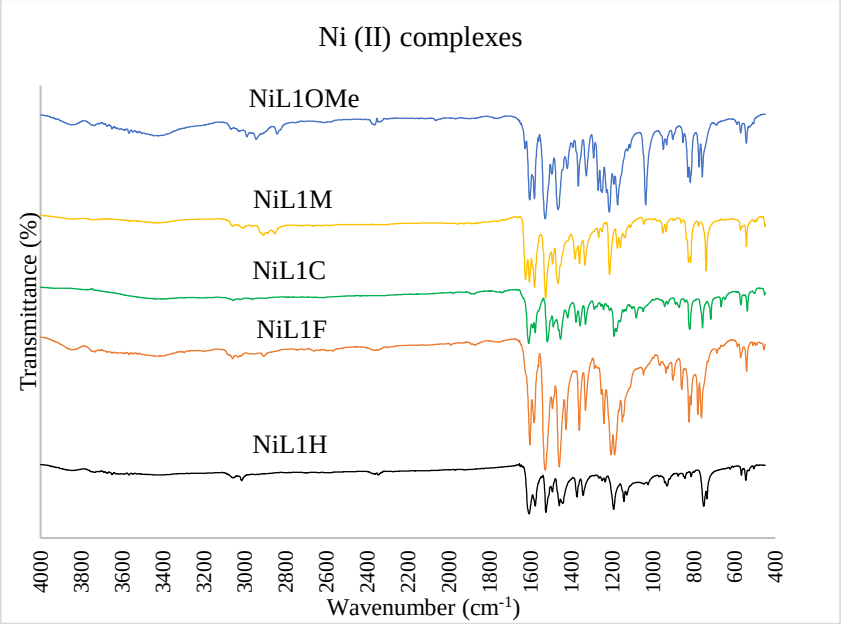

Figure 2. IR spectra of Ni(II) complexes.

Table 2. FT-IR data of Pd(II) and Ni(II) complexes.

Compounds	Wavenumber, ν (cm^{-1})				
	C=N	C–N	C–O (phenol)	M–N	M–O
PdL1H	1607 (*s*)	1180 (*m*)	1051 (*w*)	534 (*w*)	461 (*w*)
NiL1H	1607 (*s*)	1192 (*m*)	1045 (*w*)	526 (*w*)	494 (*w*)
PdL1F	1606 (*s*)	1146 (*m*)	1047 (*w*)	583 (*w*)	481 (*w*)
NiL1F	1602 (*s*)	1150 (*m*)	1047 (*w*)	521 (*w*)	474 (*w*)
PdL1C	1607 (*s*)	1169 (*w*)	1048 (*w*)	523 (*w*)	484 (*w*)
NiL1C	1609 (*s*)	1190 (*w*)	1048 (*w*)	519 (*w*)	471 (*w*)
PdL1M	1608 (*s*)	1158 (*w*)	1045 (*w*)	516 (*w*)	463 (*w*)
NiL1M	1605 (*s*)	1159 (*m*)	1045 (*w*)	521 (*w*)	461 (*w*)
PdL1OMe	1607 (*s*)	1171 (*w*)	1036 (*s*)	533 (*w*)	478 (*w*)
NiL1OMe	1603 (*s*)	1173 (*m*)	1036 (*s*)	536 (*w*)	498 (*w*)

Note: *s* -strong; *m* -medium; *w* -weak

The existence of benzene rings as part of the chemical structure of ligands and complexes was suggested by the appearance of weak ν(CH) sp^2 stretching vibrations in the range of 3014–3086 cm^{-1} and medium ν(C=C) stretching vibrations in the range of 1524–1588 cm^{-1}. The benzene rings also gave rise to two medium or weak vibrations of ν(CH) bending in the vicinity of 727–787 cm^{-1} and 824–874 cm^{-1}. These wave numbers suggest that there were two substituents attached to the ring structure.

There were two new weak peaks that appeared in the spectra of the metal complexes in the range of 461–498 cm^{-1} and 516–583 cm^{-1}, which were assignable to M–O and M–N, respectively. These values are in concordance with the wavenumbers reported by Nasaruddin *et al.* [30]. These bands signify the complexation between metal and ligand through azomethine nitrogen and phenolic oxygen [31]. The frequency of the M–N bands was found to be higher than that of the M–O bands as the former had lower molecular weights, and this obeys Hooke's law [32-33]. These metal-ligand bonds mostly appear as very weak bands as they are very sensitive towards substituent effects [34-35].

^{1}H and ^{13}C NMR Spectra

The ^{1}H and ^{13}C NMR spectra of the complexes in DMSO-d_6 were recorded. **Table 3** shows the ^{1}H NMR data of the Pd(II) and Ni(II) complexes. OH appeared as a singlet at 12.62–13.09 ppm in the spectra of the free ligands. Here, these hydroxyl protons were found in the downfield region, likely due to the formation of hydrogen bonding [23, 36] with azomethine nitrogen, as well as the deshielding effect of oxygen. The absence of OH peaks in the spectra of both complexes supports the infrared evidence that

coordination to the metal centres was established through deprotonation of the hydroxyl groups [26].

The azomethine proton, HC^7=N, appeared as a singlet in the region of 8.57–8.87 ppm for all free ligands. In the PdL1H and NiL1H spectra, this signal was found in the downfield region with respect to L1H, at 8.49 and 8.22 ppm, respectively. This supports the shifting of the azomethine peak in the FTIR spectra, which suggested the involvement of azomethine nitrogen in the coordination to metal centres [29], [37]. However, the peak was discovered to be in the upfield region with respect to their parent ligands, ranging from 8.69 to 9.21 ppm in other palladium(II) and nickel(II) complexes. The substituents attached to the aromatic carbon of the ligands may have contributed to this trend [38, 39].

The chemical shifts of aromatic protons in the free ligands appeared as multiplets in the range of 6.87–7.45 ppm. This is in agreement with the chemical shifts reported by Ansari *et al*. [40-41]. These hydrogens experience the shielding effect of diamagnetic anisotropy caused by circulating π electrons in the aromatic rings [33]. The signals of these aromatic protons were found at 6.64–8.33 ppm in the complexes. The different chemical shifts of these protons indicate the complexation between the metal ions and ligands. Their coupling constant values, 1–3 and 6–9 Hz, suggest the presence of *ortho* and *meta* hydrogens.

Table 3. ^{1}H NMR data of the Pd(II) and Ni(II) complexes.

Compounds	Assignment, δ (ppm)								
	HC^7=N	C^2-H (Ar)	C^9-H (Ar)	C^4-H (Ar)	C^{10}-H (Ar)	C^3-H (Ar)	C^5-H (Ar)	Ar-CH_3	Ar-OCH_3
PdL1H	8.49 (*s*, 2H)	6.68 (*ddd*, 2H, 7.9, 6.7, 1.0 Hz)	7.41 (*m*, 2H)	7.32 (*dd*, 2H, 6.3, 3.2 Hz)	7.41 (*m*, 2H)	7.41 (*m*, 2H)	7.86 (*m*, 2H)	-	-
NiL1H	8.22 (*s*, 2H)	6.64 *(td*, 2H, 7.2, 0.8 Hz)	7.17 (*d*, 2H, *J*=8.7 Hz)	7.22 *(dd*, 2H, 6.2, 3.2 Hz)	7.30 *(d*, 2H, 7.2 Hz)	7.30 *(d*, 2H, 7.2 Hz)	7.71 *(dd*, 2H, 6.2, 3.3 Hz)	-	-
PdL1F	9.18 (*s*, 2H)	7.03 (*dd*, 2H, 9.4, 4.8 Hz)	7.38 (*ddd*, 2H, 9.3, 7.8, 3.3 Hz)	-	7.52 (*dd*, 2H, 9.7, 3.3 Hz)	7.48 (*dd*, 2H, 6.3, 3.3 Hz)	8.28 (*dd*, 2H, 6.3, 3.3 Hz)	-	-
NiL1F	8.90 (*s*, 2H)	6.90 (*dd*, 2H, 9.4, 4.6 Hz)	7.18 (*m*, 2H)	-	7.35 (*m*, 2H)	7.35 (*m*, 2H)	8.09 (*dd*, 2H, 6.3, 3.4 Hz)	-	-
PdL1C	9.21 (*s*, 2H)	6.73 (*m*, 2H)	7.03 (*d*, 2H, 8.4 Hz)	-	7.46 (*m*, 2H)	7.75 (*dd*, 2H, 8.1, 1.7 Hz)	8.36 (*m*, 2H)	-	-
PdL1M	9.13 (*s*, 2H)	6.95 (*d*, 2H, 6.7 Hz)	7.44 (*dd*, 2H, 6.3, 3.2 Hz)	-	7.51 (*s*,2H)	7.29 (*dt*, 2H, 8.8, 2.3 Hz)	8.33 (*dd*, 2H, 6.4, 3.4 Hz)	2.26 (*s*, 6H)	-
NiL1M	8.69 (*s*, 2H)	6.83 (*d*, 2H, 3.3 Hz)	7.27 (*dd*, 2H, 6.2, 3.2 Hz)	-	7.27 (*dd*, 2H, 6.2, 3.2 Hz)	7.11 (*dd*, 2H, 8.7, 2.2 Hz)	8.06 (*dd*,2H, 6.2, 3.4 Hz)	2.22 (*s*, 6H)	-
PdL1OMe	9.21 (*s*, 2H)	6.99 (*d*, 2H, 9.3 Hz)	7.25 (*d*, 2H, 3.2 Hz)	-	7.46 (*dd*, 2H, 6.3, 3.3 Hz)	7.18 (*dd*, 2H, 9.2, 3.3 Hz)	8.32 (*dd*, 2H, 6.4, 3.3 Hz)	-	3.79 (*s*, 6H)
NiL1OMe	8.78 (*s*, 2H)	6.87 (*d*, 2H, 3.0 Hz)	7.06 (*d*, 2H, 9.3 Hz)	-	7.28 (*dd*, 2H, 6.3, 3.2 Hz)	6.99 (*dd*, 2H, 9.1, 2.9 Hz)	8.07 (*dd*, 2H, 6.1, 3.4 Hz)	-	3.73 (*s*, 6H)

Note: (s) = singlet; (*d*) = doublet; (*dd*) = doublet of doublets; (*ddd*) = doublet of doublet of doublets; (*t*) = triplet; *(m)* = multiplet; N.D. = not detected; Ar = aromatic

The azomethine carbon, C=N was found in the range of 155.70–161.37 ppm in all the free ligands, with no significant influence of substituents. In the complexes, it appeared at upfield regions in the range of 152.50–156.50 ppm. This indicates that complexation had occurred between the metal centre and azomethine nitrogen [42], which further supports the FTIR data. Complexation between the metal centres and phenolic oxygen, on the other hand, could be observed through the shifting of C–OH/C–O signals. The signal of C–OH was higher than that of C=N due to the higher electro-negativity of oxygen (3.44) compared to nitrogen (3.04) on Pauling's scale**.**

Aromatic carbons in the compounds were seen in the range of 115.32–142.82 ppm in the free ligands and at 114.86–143.60 ppm in the complexes. The peak of the aromatic carbon, C^4–H(Ar) was found further downfield in L1F and L1OMe with respect to its peak in other ligands due to the presence of the electro-negative elements fluorine, F (3.98) and oxygen, O (3.44) next to the carbon. The shifting of aromatic carbons downfield and upfield suggests complexation between metals and ligands. The presence of a methyl group, CH_3 and a methoxy group, OCH_3 in L1M and L1OMe were detected at ~20.00 ppm and 55.99 ppm, respectively.

UV-Visible Spectra

In general, intra-ligand electronic transitions have three main characteristic absorption bands, i.e., π–π*(C=C), π–π*(C=N) and n–π*(C=N). Two weak to medium peaks of π–π*(C=C), were observed at 206–224 nm and 230–241 nm in the ligands. The weak to medium absorption bands of π–π*(C=N) were observed at 268–274 nm in the ligands. The medium to strong peaks of n–π* (C=N) were discovered at higher wavelengths, in the vicinity of 331–356 nm in the ligands. This band indicates that there is a transition of an electron from a nitrogen lone pair to the π* of imine group [43]. The electronic transition could also be assumed to have occurred from the non-bonding n orbital of the imine nitrogen to the anti-bonding π orbital [44, 45]. The λ_{max} of n–π* (C=N) was lower than the λ_{max} of π–π* (C=N) as the energy needed to excite a non-bonding, n electron is lower than that from a π orbital. Energy is in inverse proportion to wavelength ($\Delta E = hc/\lambda$).

The main characteristic peaks in the ligands were also observed in the complexes, but with some differences. Two absorption bands of π–π*(C=C) experienced a red shift (bathochromic) relative to their parent ligands at 214–237 nm and 237–257 nm in the complexes. The peak of π–π*(C=N) also experienced a bathochromic effect, shifting to a longer wavelength where the bands were seen at 289–344 nm in the L1 series complexes. These observations suggest that complexation had occurred between the Schiff base ligands and metal ions [46-47]. The results are in agreement with the values and trends reported by Sankara et al. (2023) [48].

The absorption bands of n–π*(C=N) were observed to exhibit the bathochromic shift, at 353–402 nm in the complexes. The bathochromic shifts of this band occurred as a consequence of the lone electron pair donation from azomethine nitrogen to the metal (N→M) [49-50].

New peaks were found at 476–511 nm in the complexes, correspondingly attributable to ligand to metal charge transfers (LMCT) [37, 53]. These bands indicate that there was an interaction established between the imine nitrogen and the metal centre, forming a dative covalent bond where the electrons moved from the π orbital of the ligand to the *d* orbital of the metal [36]. UV-Visible spectra of PdL1C and NiL1C could not be obtained due to solubility limitations.

λ_{max} assignable to *d-d* transitions could not be detected in the spectra of the complexes as this falls under Laporte forbidden transitions, where the compounds were centrosymmetric. The peaks, if they existed, would appear as very weak peaks with low molar absorptivity at a wavelength of more than 600 nm in the visible region. The absence of these peaks may likely be concealed by strong ligands and charge transfer bands in the UV region [52].

Table 4. UV-Vis data of the Pd(II) and Ni(II) complexes.

Compounds	Band Assignment, λ_{max}, nm (ε, L mol^{-1} cm^{-1})			
	π–π* (benzene)	π–π* (C=N)	n–π* (C=N)	LMCT
PdL1H	218 (11930), 247 (10955)	315 (6433)	353 (6299)	476 (3419)
NiL1H	233 (3655), 259 (17291)	308 (6504)	376 (9543)	478 (3022)
PdL1F	214 (7930), 239 (5150)	317 (3666)	384 (1548)	484 (2309)
NiL1F	234 (6037), 257 (6701)	289 (3096)	379 (4344)	488 (1436)
PdL1M	219 (149260), 251 (12607)	317 (7612)	386 (2727)	485 (4082)
NiL1M	237 (17761), 261 (22145)	294 (8902)	379 (12092)	489 (3738)
PdL1OMe	221 (14612), 246 (10895)	343 (6965)	399 (2430)	510 (3976)
NiL1OMe	221 (2332), 247 (9162)	344 (5708)	402 (2007)	511 (3293)

Ligands were seen as yellow solutions in MeCN, indicating the characteristic of strong-field ligands of Schiff bases due to the existence of C=N chromophores in the ground state [53]. Strong-field ligands generally induce the formation of square-planar geometry, and this was observed in the palladium(II) and nickel(II) complexes studied in this research.

Catalytic Activity

Under optimized reaction conditions (KOH, 140 °C and 2.0 mmol %), the reactions catalysed by various palladium(II) and nickel(II) complexes were carried out smoothly to afford the product in moderate to high yields; the results are presented in **Table 5**. It is apparent that the palladium(II) complexes performed better than the nickel(II) complexes. This is in line with the results reported by Esmaeilpour, Javidi, Dodeji, & Abarghoui, where palladium converted a higher percentage of reactant than nickel. Nonetheless, the catalytic performance of the nickel(II) complexes was quite decent and better than those previously reported [54, 55]. The lowest percentage conversion was 78 % and the highest conversion was 91 %. Metal centres play a more important role in catalytic activities than ligands. Nonetheless, the presence of ligands should not be neglected as they play a huge role in accustoming the rate of some or all of the catalytic steps, like oxidative addition, insertion, transmetalation and reductive elimination [56]. In fact, the deposition of palladium black, a marker of deactivation of the catalytic site of the metal, is known to happen rather quickly in ligand-less catalysis [56, 57].

There were two control experiments in this investigation. The reaction without any Pd(II) and Ni(II) species, i.e., the negative control, showed no conversion of iodobenzene. The positive control using palladium(II) acetate as a catalyst showed the highest conversion of 100 % after 3 hours of reaction time. However, the formation of palladium black was detected at 120 °C, signalling the decomposition of palladium(II) acetate. There was no formation of palladium black in any of the reactions catalysed by the complexes. This showed that the ligands acted as effective stabilizers to the active catalytic sites of Pd(II) and Ni(II).

The electronic profile of the ligand appears to play a significant role in catalytic activities in the coupling reaction, such that complexes with ligands bearing electron withdrawing groups (namely F, Cl, and NO_2) outdid the performance of those with electron donating substituents such as CH_3 and OCH_3. This was more pronounced in nickel(II) complexes where NiL1F converted the highest percentage of iodobenzene (91 %) after 12 hours of reaction. The presence of electron withdrawing substituents increases the acidity of hydrogen in metal-acetylide complexes, facilitating an elimination reaction. Furthermore, its presence in the structure may have an inductive effect which leads to facile oxidative addition.

Antibacterial Activity

The MIC and MBC values of the 15 compounds against MRSA ATCC 43300, MRSA NCTC 12494 and MSSA ATCC 12600 are shown in **Table 6**. L_1Me showed the most promising anti-MRSA and anti-MSSA activity, with both MIC and MBC values of 3 µg/ml against the tested strains. L1C, L1F and L1N showed MIC and MBC values between 50-100 µg/ml, while the remaining compounds gave MIC and MBC values greater than the highest tested concentration of 200 µg/ml.

Table 5. Percentage conversion of iodobenzene using different catalysts.

Complexes	Catalyst	3 h	6 h	12 h
Palladium(II) complexes	PdL1H	100	100	100
	PdL1F	100	100	100
	PdL1C	100	100	100
	PdL1M	100	100	100
	PdL1OMe	100	100	100
Nickel(II) complexes	NiL1H	67	71	78
	NiL1F	80	87	91
	NiL1C	73	80	83
	NiL1M	75	81	89
	NiL1OMe	73	80	81

Table 6. Minimum inhibitory concentration (MIC) and minimum bactericidal concentration (MBC) of the compounds against methicillin-resistant *Staphylococcus aureus* (ATCC 43300 and NCTC 12493) and methicillin-sensitive *Staphylococcus aureus* (ATCC 12600) strains.

SAMPLE	MRSA 43300		MRSA 12493		MSSA 12600	
	MIC	MBC	MIC	MBC	MIC	MBC
#1 – L1C	200	200	200	200	200	200
#2 – L1F	100	100	100	100	100	100
#3 – L1Me	3	3	3	3	3	3
#4 – L1OMe	>200	>200	>200	>200	>200	>200
#5 – L1N	50	50	100	200	100	200
#11 – NiL1C	>200	>200	>200	200	>200	>200
#12 – NiL1F	>200	>200	>200	>200	>200	>200
#13 – NiL1Me	>200	>200	>200	>200	>200	>200
#14 – NiL1OMe	>200	>200	>200	>200	>200	>200
#15 – NiL1N	>200	>200	>200	>200	>200	>200
#21 – PdL1C	>200	>200	>200	>200	>200	>200
#22 – PdL1F	>200	>200	>200	>200	>200	>200
#23 – PdL1Me	>200	>200	>200	>200	>200	>200
#24 – PdL1OMe	>200	>200	>200	>200	>200	>200
#25 – PdL1N	>200	>200	>200	>200	>200	>200

CONCLUSION

Both Pd(II) and Ni(II) Schiff base complexes were prepared via condensation reactions. The formation of the metal complexes was verified through physico-chemical and spectroscopic analysis. The shifting of significant peaks in FTIR, ^{1}H and ^{13}C NMR, and UV–Vis spectra indicated that complexation had taken place through deprotonation of the phenolic proton and shifting of the azomethine nitrogen. Pd(II) complexes showed greater catalytic performance in the Sonogashira reaction under optimum conditions, compared to Ni(II) complexes. In the antimicrobial study, L1Me showed good potential as an anti-MRSA and anti-MSSA agent due to its low MIC and MBC values.

ACKNOWLEDGEMENTS

The authors would like to acknowledge the Ministry of Higher Education, Malaysia and Universiti Teknologi MARA for the financial support through research grant no. 600-IRMI/MyRA 5/3/BESTARI (034/2017), scholarship and research facilities.

REFERENCES

1. Dhilshath Raihana, H., Karthick, K., Shankar, T., Kamalesu, S., Anish Babu, A. and Swarnalatha, K. (2022) A new tetradentate Schiff base of N,N'-bis(3,5-diiodosalicylidene)-1,2-phenylenediamine: Spectral aspects, Hirshfield surfaces, DFT computations and molecular docking. *J. Mol. Struct.*, **1264**, 133217.

2. Asatkar, A. K., Tripathi, M. and Asatkar, D. (2020) Salen and Related Ligands. In *Stability and Applications of Coordination Compounds*, 1–20.

3. Mazzoni, R., Roncaglia, F. and Rigamonti, L. (2021) When the Metal Makes the Difference: Template Syntheses of Tridentate and Tetradentate Salen-Type Schiff Base Ligands and Related Complexes. *Crystals*, **11**, 483.

4. Baleizão, C. and Garcia, H. (2006) Chiral salen complexes: An overview to recoverable and reusable homogeneous and heterogenous catalysts. *Chem. Rev.*, **106**, 9, 3987–4043.

5. Kargar, H., *et al.* (2022) Synthesis, spectral characterization, crystal structures, biological activities, theoretical calculations and substitution effect of salicylidene ligand on the nature of mono and dinuclear Zn(II) Schiff base complexes. *Polyhedron*, **213**, 115636, July 2021.

6. Sathya, M. and Venkatachalam, G. (2022) Synthesis, Structural Characterization and Catalytic Activities of Palladium(II) Schiff base Complexes Containing Tetradentate N2O2 & N2S2 Donor Ligands. *Int. J. Multidiscip. Res.*, **04(04)**, 417–428.

7. Wang, J., Blaszczyk, S. A., Li, X. and Tang, W. (2021) Transition Metal-Catalyzed Selective Carbon-Carbon Bond Cleavage of Vinylcyclopropanes in Cycloaddition Reactions. *Chem. Rev.*, **121(1)**, 110–139.

8. Bahron, H., Ahmad, S. N., Tajuddin, A. M. and Kadir, S. I. A. Y. S. A. (2017) Substituent effect on catalytic activity of palladium(II) schiff base complexes for sonogashira reaction. *Pertanika J. Sci. Technol.*, **25**, S4, 115–124.

9. Talukder, M. M., *et al.* (2020) Ligand steric effects of α-diimine nickel(II) and palladium(II) complexes in the suzuki-miyaura cross-coupling reaction. *ACS Omega*, **5**, 37, 24018–24032.

10. Wang, Z., Zheng, T., Sun, H., Li, X., Fuhr, O. and Fenske, D. (2018) Sonogashira reactions of alkyl halides catalyzed by NHC [CNN] pincer nickel(II) complexes. *New J. Chem.*, **42(14)**, 11465–11470.

11. Nair, P. P., Philip, R. M. and Anilkumar, G. (2021) Nickel catalysts in Sonogashira coupling reactions. *Org. Biomol. Chem.*, **19(19)**, 4228–4242.

12. Guadouri, H. A., Merzougui, M., Hannachi, D., Ali, M. A. and Ouari, K. (2021) Unsymmetrical salen nickel (II) complex embracing phenol bridge: X-ray structure, redox investigation, computational calculations, antimicrobial and catalytic activities. *J. Mol. Struct.*, **1242**, 130809.

13. Sovari, S. N. and Zobi, F. (2020) Recent Studies on the Antimicrobial Activity of Transition Metal Complexes of Groups 6–12. *Chem.*, **2(2)**, 418–452.

14. Nyawade, E. A., Onani, M. O., Meyer, S. and Dube, P. (2020) Synthesis, characterization and antibacterial activity studies of new 2-pyrral-L-amino acid Schiff base palladium (II) complexes. *Chem. Pap.*, **II.**

15. Kumar, R., *et al.* (2023) Recent advances in synthesis of heterocyclic Schiff base transition metal complexes and their antimicrobial activities especially antibacterial and antifungal. *J. Mol. Struct.*, **1294**, P2, 136346.

16. Raj, P., Singh, A., Singh, A. and Singh, N. (2017) Syntheses and Photophysical Properties of Schiff Base Ni(II) Complexes: Application for Sustainable Antibacterial Activity and Cytotoxicity. *ACS Sustain. Chem. Eng.*, **5(7)**, 6070–6080.

17. Ahmad, S. N., Bahron, H. and Tajuddin, A. M. (2018) Tetradentate Palladium(II) Salophen complexes: Synthesis, characterization and catalytic activities in copper-free Sonogashira coupling reaction. *Int. J. Eng. Technol.*, **7(3)**, 15–19.

18. Whangbo, M. H., Koo, H. J. and Kremer, R. K. (2021) Spin exchanges between transition metal ions governed by the ligand P-orbitals in their magnetic orbitals. *Molecules*, **26(3)**, 1–26.

19. Yousif, E., Majeed, A., Al-Sammarrae, K., Salih, N., Salimon, J. and Abdullah, B. (2013) Metal complexes of Schiff base: Preparation, characterization and antibacterial activity. *Arab. J. Chem.*, **10**, S1639–S1644.

20. Aslam, M., *et al.* (2021) Synthesis, characterization, biological screening and determination of stability constants of N,N′-Bis[1-(4-chlorophenyl)ethylidene] ethane-1,2-diamine. *SN Appl. Sci.*, **3(1)**, 1–7.

21. Raman, N., Kulandaisamy, A., Thangaraja, C., Manisankar, P., Viswanathan, S. and Vedhi, C. (2004) Synthesis, structural characterisation and electrochemical and antibacterial studies of Schiff base copper complexes. *Transit. Met. Chem.*, **29(2)**, 129–135, Mar. 2004.

22. Aggoun, D., *et al.* (2020) New nickel (II) and copper (II) bidentate Schiff base complexes, derived from dihalogenated salicylaldehyde and alkylamine: Synthesis, spectroscopic, thermogravimetry, crystallographic determination and electrochemical studies. *Polyhedron*, **187**, 114640.

23. Ahmad, S. N., Bahron, H., Tajuddin, A. M. and Ramasamy, K. (2019) Tetradentate phenolic Schiff base ligands derived from aromatic diamine and their nickel (II) complexes: Synthesis, characterization, and in vitro anticancer screening. *Malaysian J. Fundam. Appl. Sci.*, **15(4)**, 613–616.

24. Oruma, U. S., *et al.* (2021) Synthesis, biological and in silico studies of a tripodal schiff base derived from 2,4,6-triamino-1,3,5-triazine and its trinuclear Dy(III), Er(III), and Gd(III) salen capped complexes. *Molecules*, **26(14)**, 1–15.

25. Prabhu, R. N. and Lakshmipraba, J. (2017) A nickel(II) thiosemicarbazonato complex: synthesis, structure, electrochemistry, and application in catalytic coupling of terminal alkynes with arylboronic acids. *Transit. Met. Chem.*, **42(7)**, 579–585.

26. Pratihar, J. L., Mandal, P., Lai, C. K. and Chattopadhyay, S. (2019) Tetradentate amido azo Schiff base Cu(II), Ni(II) and Pd(II) complexes: Synthesis, characterization, spectral properties, and applications to catalysis in C–C coupling and oxidation reaction. *Polyhedron*, **161**, 317–324.

27. Hille, A., *et al.* (2009) [N,N′-Bis(salicylidene)-1, 2-phenylenediamine]metal complexes with cell death promoting properties. *J. Biol. Inorg. Chem.*, **14(5)**, 711–725.

28. Solihah, S., *et al.* (2023) Synthesis, structural elucidation, Hirshfeld surface analysis and cyto-toxicity studies of homometallic dinuclear Cu (II), Ni (II) and Zn (II) Schiff base complexes derived from m- phenylenediamine. *J. Mol. Struct.*, **1294**, P1, 136386.

29. Kargar, H., *et al.* (2022) Pd(II) and Ni(II) complexes containing ONNO tetradentate Schiff base ligand: Synthesis, crystal structure, spectral characterization, theoretical studies, and use of PdL as an efficient homogeneous catalyst for Suzuki–Miyaura cross-coupling reaction. *Polyhedron*, **213**, 115622, October, 2021.

30. Nasaruddin, N. H., *et al.* (2022) Synthesis, Structural Characterization, Hirshfeld Surface Analysis, and Antibacterial Study of Pd(II) and Ni(II) Schiff Base Complexes Derived from Aliphatic Diamine. *ACS Omega*, **7(47)**, 42809–42818.

31. Rosnizam, A. N., *et al.* (2022) Palladium(II) complexes bearing N,O-bidentate Schiff base ligands: Experimental, in-silico, antibacterial, and catalytic properties. *J. Mol. Struct.*, **1260**, 132821.

32. Shaner, S. E. and Stone, K. L. (2023) Determination of Stretching Frequencies by Isotopic Substitution Using Infrared Spectroscopy: An Upper-Level Undergraduate Experiment for an In-Person or Online Laboratory. *J. Chem. Educ.*, **100**, 6, 2347–2352.

33. Pavia, D. L., Lampman, G. M., Kriz, G. S. and Vyvyan, J. R. (2015) *Introduction to Spectroscopy*, 5th edition Cengage Learning.

34. Douglas Hancock, R. (2014) Crystal Field Aspects of Vibrational Spectra. *University of Cape Town*.

35. Percy, G. C. and Thornton, D. A. (1973) Infrared spectra of N-aryl salicylaldimine complexes substituted in both aryl rings. *J. Inorg. Nucl. Chem.*, **35(7)**, 2319–2327.

36. Aranha, P. E., dos Santos, M. P., Romera, S. and Dockal, E. R. (2007) Synthesis, characterization, and spectroscopic studies of tetradentate Schiff base chromium(III) complexes. *Polyhedron*, **26(7)**, 1373–1382.

37. Turan, N., Buldurun, K., Bursal, E. and Mahmoudi, G. (2022) Pd(II)-Schiff base complexes: Synthesis, characterization, Suzuki–Miyaura and Mizoroki–Heck cross-coupling reactions, enzyme inhibition and antioxidant activities. *J. Organomet. Chem.*, 970–971, 122370.

38. Khaidir, S. S., Bahron, H., Tajuddin, A. M. and Ramasamy, K. (2022) Microwave-Assisted Synthesis, Characterization and Anticancer Activity of Tetranuclear Schiff Base Complexes. *J. Sustain. Sci. Manag.*, **17(4)**, 32–48.

39. Khoo, L. E. (1979) Azomethine proton chemical shift of Schiff bases. *Spectrochim. Acta Part A Mol. Spectrosc.*, **35(8)**, 993–995.

40. Ansari, R. M., Kumar, L. M. and Bhat, B. R. (2018) Air-Stable Cobalt(II) and Nickel(II) Complexes with Schiff Base Ligand for Catalyzing Suzuki–Miyaura Cross-Coupling Reaction. *Russ. J. Coord. Chem. Khimiya*, **44(1)**, 1–8.

41. Adeleke, A. A., Oladipo, S. D., Zamisa, S. J., Sanusi, I. A. and Omondi, B. (2023) Inorganica Chimica Acta DNA / BSA binding studies and in vitro anticancer and antibacterial studies of iso-electronic Cu (I) - and Ag (I) -pyridinyl Schiff base complexes incorporating triphenylphosphine as co-ligands. *Inorganica Chim. Acta*, **558**, 121760, July, 2023.

42. Waziri, I., Yusuf, T. L., Zarma, H. A., Oselusi, S. O., Coetzee, L. -C. C. and Adeyinka, A. S. (2023) New Palladium(II) Complexes from Halogen Substituted Schiff Base Ligands: Synthesis, Spectro-scopic, Biological Activity, Density functional theory, and Molecular Docking Investigations. *Inorganica Chim. Acta*, **II**, 121505.

43. Kargar, H., Ashfaq, M., Fallah-Mehrjardi, M., Behjatmanesh-Ardakani, R., Munawar, K. S. and Tahir, M. N. (2022) Synthesis, crystal structure, spectral characterization, theoretical and computational studies of Ni(II), Cu(II) and Zn(II) complexes incorporating Schiff base ligand derived from 4-(diethylamino)salicylaldehyde. *Inorganica Chim. Acta*, **536**, 120878.

44. Kumar, Y., *et al.* (2022) DNA/Protein binding and anticancer activity of Zn(II) complexes based on azo-Schiff base ligands. *Inorganica Chim. Acta*, **538**, 120963.

45. Gondia, N. K. and Sharma, S. K. (2018) Spectro-scopic characterization and photophysical properties of schiff base metal complex. *J. Mol. Struct.*, **1171**, 619–625.

46. Archana, B. and Sreedaran, S. (2023) Synthesis, characterization, DNA binding and cleavage studies, in-vitro antimicrobial, cytotoxicity assay of new manganese(III) complexes of N-functionalized macrocyclic cyclam based Schiff base ligands. *Polyhedron*, **231**.

47. Guangbin, W. (1999) Studies on Cu(II), Zn(II), Ni (II) and Co(II) complexes derived from two dipeptide Schiff bases. *Spectrosc. Lett.*, **32(4)**, 679–688.

48. Sankara, V., Rajendran, A., Mudradi, S. and Dhawa, S. (2023) Development of new cobalt, copper, and zinc complexes of Schiff-base ligands as prospective chemotherapeutic agents. *Polyhedron*, **245**, 116622.

49. Ghose, B. N. and Lasisi, K. M. (1986) Schiff base complexes of titanium: Reaction of titanium(IV) tetrachloride with dibasic tetradentate Schiff bases. *Synth. React. Inorg. Met. Chem.*, **16(8)**, 1121–1133.

50. Lashanizadegan, M., Asna Ashari, H., Sarkheil, M., Anafcheh, M. and Jahangiry, S. (2021) New Cu(II), Co(II) and Ni(II) azo-Schiff base complexes: Synthesis, characterization, catalytic oxidation of alkenes and DFT study. *Polyhedron*, **200**, 115148.

51. Lakshmipraba, J., Ebenezer, C., Solomon, R. V. and Venkatesan, M. (2023) Explorations on the synthesis, structure, DFT, DNA binding properties and molecular docking of tridentate Schiff base Copper (II) complexes. *Chem. Phys. Impact*, **7**, 100286.

52. Kwiatkowski, E. and Kwiatkowski, M. (1980) Unsymmetrical schiff base complexes of nickel(II) and palladium(II). *Inorganica Chim. Acta*, **42**, C, 197–202.

53. Atkins, P., Overton, T., Rourke, J., Weller, M., Armstrong, F. and Hagerman, M. (2010) *Inorganic chemistry*.

54. Hegade, S., Jadhav, Y., Chavan, S., Mulik, G. and Gaikwad, G. (2020) Catalytic assay of Schiff base Co(II), Ni(II), Cu(II) and Zn(II) complexes for N-alkylation of heterocycles with 1,3-dibromo-propane. *J. Chem. Sci.*, **132(1)**, 1–7.

55. Esmaeilpour, M., Javidi, J., Dodeji, F. N. and Abarghoui, M. M. (2014) M(II) Schiff base complexes (M= zinc, manganese, cadmium, cobalt, copper, nickel, iron, and palladium) supported on superparamagnetic Fe3O4 @ SiO2 nanoparticles : synthesis, characterization and catalytic activity for Sonogashira – Hagihara coupli. *Transit. Met. Chem.*, **39**, 797–809.

56. Farina, V. (2004) High-turnover palladium catalysts in cross-coupling and Heck chemistry: A critical overview. *Adv. Synth. Catal.*, **346**, 13–15, 1553–1582.

57. Epifanov, E. O., Shubnyi, A. G., Minayev, N. V., Rybaltovskiy, A. O., Yusupov, V. I. and Parenago, O. P. (2020) Synthesis of Heterogeneous Catalysts by Laser Ablation of Metallic Palladium with Deposition on Alumina in Supercritical Carbon Dioxide. *Russ. J. Phys. Chem. B*, **14(7)**, 1103–1107.